

Tribological characterization of nanoparticle filled PTFE: Wear-induced crystallinity increase and filler accumulation

L. F. Tóth^{1,2}, G. Szébenyi^{2*}, J. Sukumaran¹, P. De Baets^{1,3}

¹Soete Laboratory, Department of Electromechanical, Systems and Metal Engineering, Ghent University, Technologiepark Zwijnaarde 46, B-9052 Zwijnaarde, Belgium

²Department of Polymer Engineering, Faculty of Mechanical Engineering, Budapest University of Technology and Economics, Műegyetem rkp. 3, H-1111 Budapest, Hungary

³FlandersMake@UGent – Core lab EEDT-DC, Belgium

Received 4 May 2021; accepted in revised form 8 June 2021

Abstract. The present research aims to clarify the friction and wear behavior, the transfer layer formation, and the wear mechanism of mono-filled polytetrafluoroethylene (PTFE). A well-known limitation of PTFE is the low wear resistance, which can be surpassed with the use of micro- or nanoparticles. The applied fillers were graphene, alumina (Al₂O₃), boehmite alumina (BA80), and hydrotalcite (MG70). The samples were produced by room temperature pressing – free sintering method. All specimens were tested with a pin-on-disc tribo-tester in dry contact condition against 42CrMo4 steel disc counterface with 3 MPa contact pressure and 0.1 mm/s sliding speed. PTFE filled with 4 wt% Al₂O₃ achieved the highest wear resistance; the increase was more than two orders of magnitude compared to the neat PTFE. This improvement comes from the protective transfer layer formation due to the Al₂O₃ and the iron-oxide accumulation on the polymer contact surface. Significant wear-induced crystallinity was also registered, which originated from the mechanical chain scission of the PTFE molecular chains during the wear process.

Keywords: polymer composites, nanoparticle-filled PTFE, filler accumulation, wear-induced crystallinity, sliding wear

1. Introduction

Nanoparticles are widely used fillers in thermoplastics as they can improve the mechanical and thermal properties, flame retardancy, and wear resistance of the matrix materials [1–5]. Polytetrafluoroethylene (PTFE) is well-known in tribological applications, as it has high thermal stability, excellent chemical resistance, low coefficient of friction, and good self-lubricating property compared to other semi-crystalline thermoplastics. This polymer is widely used both as a filler or as a matrix material. A remarkable challenge with PTFE is the low wear resistance. When PTFE is used as a matrix material, for example, in sliding bearings [6], besides the high wear rate, another limitation is the low mechanical performance.

In these application areas, surpassing the mechanical performance of neat PTFE is a requirement. The use of fillers such as fibers and micro- or nanoparticles can enhance the mechanical features and the wear resistance as well [7, 8].

Graphene and alumina (Al₂O₃) nanofillers can enhance the wear resistance of PTFE by 2 to 3 orders of magnitude [9–11]. The reason for this significant improvement is still an open question. Harris *et al* [12]. investigated alumina-filled PTFE, and they explained the remarkable enhancement of the wear rate with the role of tribo-chemical reactions during the wear process. According to the present understanding, the long PTFE chains undergo mechanical chain scission during wear, whereby under the action of air

*Corresponding author, e-mail: szebenyi@pt.bme.hu
© BME-PT

(oxygen) and humidity, terminal carboxyl groups (COOH) form on the PTFE chain fragments (*in situ* ‘carboxyl functionalization’) [10, 12]. These *in situ* formed carboxyl functional groups formed on the PTFE chain during wear can participate in complex formation with the metal counterfaces. When the filler is alumina, the carboxyl groups of PTFE react with the atoms of alumina particles [12].

Fillers which have a large number of functional groups can be beneficial in sliding wear applications. The functional groups of the nanofillers can participate in complex formation with the *in situ* formed ‘functionalized’ PTFE carboxyl groups, forming a more durable and adequate transfer layer. According to this hypothesis, boehmite alumina (AlO(OH), BA80) and hydrotalcite (MG70) are promising fillers in thermoplastic matrices as they have a high number of functional groups [13–15]. Karger-Kocsis and coworkers [14, 16] reported that boehmite has a positive influence on the mechanical properties, thermal stability, and scratch-resistance of polymers. The functionalization of other fillers, e.g., graphene/carbon nanotubes, also shown promising results [17]. BA80 and MG70 fillers in combination with PTFE have not been extensively investigated; in this way, we lack a thorough understanding of this material. Besides the tribo-chemical reactions, the wear rate is also affected by some other material features such as the physical, mechanical, thermal, and morphological properties. For a better understanding, a well-detailed material characterization of our developed materials was also performed in our previous research [18, 19].

The present research work is focusing on the friction and wear-characterization of nanoparticle-filled PTFE and the fundamental understanding of the wear mechanism and transfer layer formation. Two important factors, such as the wear-induced crystallization and the filler accumulation on the polymer contact surfaces, are also investigated.

2. Materials and methods

2.1. Materials

3M™ Dyneon™ TFM™ 1700 polytetrafluoroethylene (PTFE) powder was used as a matrix material with ~25 μm average particle size. It was produced by 3M Company (Minnesota Mining and Manufacturing Company, Maplewood, Minnesota, U.S.). The used graphene was xGnP® Graphene Nanoplatelets

Grade M from XG Sciences (Lansing, Michigan, U.S.) with ~25 μm average particle size. The 1015WW alpha-alumina (Al₂O₃) with 99.5% purity was produced by Nanostructured & Amorphous Materials Inc. (Houston, Texas, U.S.). The average particle size was between 27 and 43 nm. The boehmite alumina (aluminum hydroxide oxide-AlO(OH)) was Disperal® 80 (BA80) from Sasol (Johannesburg, South Africa) with ~35 μm average particle size and ~80 nm average crystallite size. Al₂O₃ content of BA80 was 80%. Pural® MG70 hydrotalcite (MG70) from Sasol (Johannesburg, South Africa) has a double-layered metal hydroxide structure including magnesium and aluminum hydroxides (70:30, respectively). It had ~45 μm average particle size.

2.2. Production protocol and properties of the unfilled/filled PTFE samples

Table 1 shows the developed unfilled and filled PTFE materials. For the blending of the powders, intensive dry mechanical stirring was applied. This blending method is a less hazardous and more environment-friendly alternative compared to solvent blending. Stirring was done by a rotating blade grinder (180 W power) with 30 seconds of stirring time. The used production technique was room temperature pressing – free sintering method for all of the introduced materials. The pressing was carried out at room temperature with a Zwick Z250 universal tester (Zwick Roell Group, Ulm, Germany). The pressing speed was 2 mm/min until reaching 12.5 MPa pressure, where 3 minutes of dwelling time was held at the same level of pressure. The sintering cycle included a 90 °C/h heating rate from room temperature to 370 °C, a 2 h dwelling time at 370 °C temperature, and a 30 °C/h cooling rate. The sintering procedure was carried out in an oven, in air atmosphere. Alumina and MG70 filled PTFE-based materials were produced only with 1 and 4 wt% filler content as according to our previous TGA and FTIR measurements; these fillers cause a thermal instability during the sintering process at higher filler content [18]. PTFE with 0.25 wt% graphene filler content was also investigated as graphene has a high volume ratio due to its low density. The size of the pressed disc samples was the following: 120 mm diameter and 4 mm thickness. All of the wear test specimens (8 mm diameter) were milled from these disc samples.

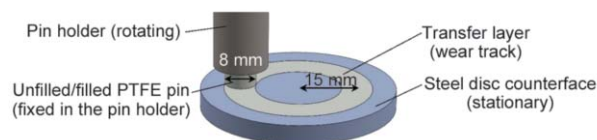
Table 1. The developed neat PTFE and PTFE-based materials.

Materials	Matrix	Filler	Filler content [wt%]
PTFE	PTFE	–	–
PTFE/graphene-0.25	PTFE	Graphene	0.25
PTFE/graphene-1	PTFE	Graphene	1
PTFE/graphene-4	PTFE	Graphene	4
PTFE/graphene-8	PTFE	Graphene	8
PTFE/graphene-16	PTFE	Graphene	16
PTFE/Al ₂ O ₃ -1	PTFE	Alumina (Al ₂ O ₃)	1
PTFE/Al ₂ O ₃ -4	PTFE	Alumina (Al ₂ O ₃)	4
PTFE/BA80-1	PTFE	Boehmite alumina (BA80)	1
PTFE/BA80-4	PTFE	Boehmite alumina (BA80)	4
PTFE/BA80-8	PTFE	Boehmite alumina (BA80)	8
PTFE/BA80-16	PTFE	Boehmite alumina (BA80)	16
PTFE/MG70-1	PTFE	Hydrotalcite (MG70)	1
PTFE/MG70-4	PTFE	Hydrotalcite (MG70)	4

2.3. Tribological characterization

2.3.1. Wear tests

Tribological characterization was performed by a Wazau TRM 1000 tribometer from Dr. Ing. Georg Wazau Mess- und Prüfsysteme GmbH, Berlin, Germany. The normal force can be applied by counterweights with a drive-spindle system in the range of 5–1000 N. As the potential application areas for the developed composites can be sliding bearings or guide rings, the applied lab-scale tribotests tried to represent these dry, sliding wear conditions. Also, the application of these standard tests makes the comparison with other research results easier. The mode and type of the applied motion is continuous sliding motion. The applied configuration was pin-on-disc with a rotating cylindrical polymer pin and stationary steel disc counterface (Figure 1). The counterface material was 42CrMo4 (EN 1.7225), which is a widely used construction steel (*e.g.*, shafts), and in this way,

**Figure 1.** Schematic representation of wear test arrangement.

in the industry, it is a potential counterpart of the developed PTFE-based materials. The counterfaces were surface finished by turning in a spiral pattern. The advantage of this surface finishing method is that in the aspect of the rotating polymer pin, the relative surface pattern of the steel is closely the same at the wear track during the wear process as it can be seen in real conditions such as, *e.g.*, shaft in a bushing. The surface roughness was S_a $0.42 \pm 0.03 \mu\text{m}$, S_z $2.39 \pm 0.17 \mu\text{m}$ and S_q $0.52 \pm 0.03 \mu\text{m}$. In perpendicular to the spiral pattern, the surface roughness was R_a $0.39 \pm 0.06 \mu\text{m}$, R_z $2.56 \pm 0.35 \mu\text{m}$ and R_q $0.49 \pm 0.07 \mu\text{m}$ (based on 5 repetitions). The measured Vickers hardness of the steel disc counterfaces was 308 ± 2 (based on 5 repetitions). The composition of the 42CrMo4 steels is introduced in Table 2. The tested polymer pin samples had a diameter of 8 mm with 4 mm thickness, while the steel counterfaces had a diameter of 50 mm. The wear track centreline on the steel discs was at 30 mm diameter. The sliding speed was 61 rpm which corresponds to 0.1 m/s (at track centreline), while the applied normal force was 151 N which corresponds to 3 MPa contact pressure. The total sliding distance was set at up to 1000 m. The presented results (coefficient of friction and the

Table 2. Standard chemical composition of the steel disc counterfaces according to EN 10083-3:2006 standard. Acronyms are the following: carbon (C), manganese (Mn), silicon (Si), phosphorus (P), sulfur (S), chromium (Cr), molybdenum (Mo), and nickel (Ni).

Steel	C	Mn	Si	P	S	Cr	Mo	Ni
42CrMo4	0.38 0.45	0.60 0.90	max 0.40	max 0.025	max 0.035	0.90 1.20	0.15 0.30	–

wear rate) represent the average of 5 tests, and standard deviation values correspond to $\pm 1\sigma$.

The coefficient of friction is calculated during the wear test by the tribometer with Equation (1):

$$CoF = \frac{Fr}{F_N} \quad (1)$$

where CoF is the coefficient of friction [–], Fr is the friction force [N] calculated by the tribometer and F_N is the applied normal force [N] measured by the tribometer.

The friction force is calculated by the tribometer with Equation (2):

$$Fr = \frac{M}{r} \quad (2)$$

where Fr is the friction force [N], M is the torque [Nm] measured by the tribometer, and r is the radius of wear track centreline [m].

The specific wear rate of the polymers was calculated after the wear test by using Equation (3):

$$k = \frac{\Delta m}{\rho \cdot F_N \cdot d_s} \quad (3)$$

where k is the specific wear rate [mm^3/Nm], Δm is the measured mass loss [g] by a weight balance after wear test, ρ is the density of the pin sample [g/mm^3], F_N is the applied normal force [N] measured by the tribometer and d_s is the total sliding distance [m] calculated by the tribometer.

The polymer samples were not dried as the relative humidity – and in this way, the absorbed water content of the samples – is an important factor for the fillers as BA80 and MG70 contain OH functional groups. Another reason is that the potential products made from these materials (e.g., sliding bearings, guide rings, seals) are working mostly in environmental conditions. During the wear tests, the relative humidity was between 50 ± 5 RH%, while the temperature was 23 ± 2 °C. Before the wear tests, the filled/unfilled PTFE pins were cleaned with isopropanol, while the steel counterfaces were cleaned with acetone and isopropanol.

2.3.2. Transfer layer analysis

Surface topography

Taylor Hobson CCI HD non-contact optical white-light interferometer (Taylor Hobson, Leicester, United Kingdom) was used to take 3D wear maps of the samples.

Fourier-transform infrared spectroscopy (FTIR)

FTIR analyses were carried out by a Bruker Tensor 37 FTIR spectrometer (Bruker, Billerica, Massachusetts, USA) with deuterated triglycine sulfate (DTGS) detector, and Specac Golden Gate single reflection monolithic diamond attenuated total reflection (ATR) sampling system. The spectroscopic transmission range was between 4000 and 600 cm^{-1} with 4 cm^{-1} resolution in wavenumbers.

Differential scanning calorimetry (DSC)

DSC measurements were carried out with a TA Instruments Q2000 device (TA Instruments, New Castle, Delaware, USA). The protocol included a heat/cool/heat module between 0 and 370 °C temperature, with 5 °C/min heating and cooling rate. The enthalpy of fusion was evaluated between 290 and 335 °C for both of the heating cycles, while the enthalpy of crystallization was evaluated between 280 and 325 °C. Samples were placed in aluminum pans and tested in 50 ml/min nitrogen flow. The degree of crystallinity was calculated by Equation (4):

$$X = \frac{\Delta H_m - \Delta H_{CC}}{\Delta H_f \cdot (1 - \alpha)} \cdot 100 \quad (4)$$

where X is the degree of crystallinity [%], ΔH_m is the enthalpy of fusion [J/g], ΔH_{CC} is the enthalpy of cold-crystallization [J/g], ΔH_f is the enthalpy of fusion for 100% crystalline PTFE [J/g], and α is the mass fraction of the fillers [–]. As PTFE did not show any cold crystallization, ΔH_{CC} was counted as zero. The degree of crystallinity was evaluated with 69 J/g enthalpy of fusion for 100% crystalline PTFE [20].

Energy-dispersive X-ray spectroscopy (EDS)

EDS investigations were carried out with a JEOL JSM 6380LA device (JEOL, Tokyo, Japan) with 15 kV accelerating voltage, 10 sweep counts, and 0.1 ms dwell time. The sufficient electron conductivity of the samples was provided by sputtering the surface with gold (Au) in a JEOL FC-1200 device.

3. Results and discussion

3.1. Coefficient of friction

Figure 2 depicts the coefficient of friction of unfilled and filled PTFE. Besides the neat PTFE, only the friction properties of graphene and alumina-filled PTFE are available in the literature, and the tendency of the measured results are in agreement with them [9, 10].

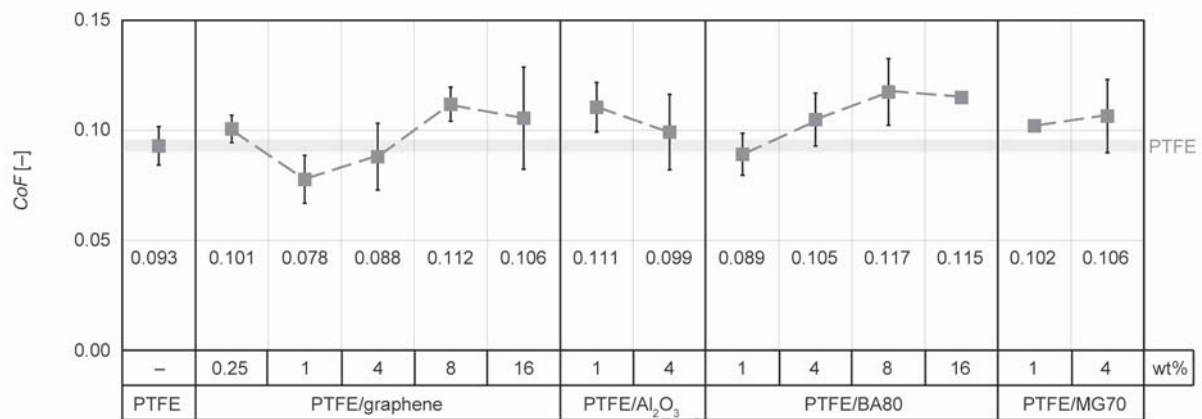


Figure 2. The dynamic coefficient of friction of unfilled/filled PTFE samples (based on 5 repetitions, standard deviations correspond to $\pm 1\sigma$). The grey transparent line displays the measured dynamic coefficient of friction of the reference neat PTFE. Dry contact, 42CrMo4 steel counterface, 3 MPa contact pressure, 0.1 m/s sliding speed, 1000 m sliding distance.

The neat PTFE had 0.093 [-] coefficient of friction against 42CrMo4 steel counterface. The most remarkable reduction was achieved by PTFE/graphene-1 material which had 0.078 [-] coefficient of friction which is ~16% lower than the reference unfilled PTFE. The coefficient of friction reduction was slighter in the case of PTFE/graphene-4 samples which had 0.088 [-] coefficient of friction. Graphene in 8 and 16 wt% filler content slightly increased the friction between the filled PTFE and the steel counterface. Al₂O₃ and MG70 filler also increased the coefficient of friction both in 1 and 4 wt%. PTFE/BA80-1 had similar friction values as unfilled PTFE; while BA80 in higher filler content increased the coefficient of friction.

Analyses of variance (ANOVA) based on both Bonferroni-Holm and Holm-Šidák methods were carried out to compare the coefficient of friction of filled PTFE materials to the reference neat PTFE. Both methods concluded that the measured differences in the coefficient of friction compared to the reference neat PTFE are not significant.

The coefficient of friction graphs of the tested materials can be seen in Figure 3. The coefficient of friction values were extracted from the full friction curves, including both the running-in period and steady-state condition. All of the materials reached steady-state friction during the applied 1000 m sliding distance. The importance of this steady-state condition is related to the reliability of the materials, and it is a good indicator of friction and wear stability. In this way, a persistent steady-state condition, besides the low coefficient of friction and low wear rate, is also a requirement in industrial applications.

All of the tested unfilled and filled PTFE samples reached the steady-state friction after ~300–400 m sliding distances (Figure 3). In the case of PTFE/graphene-4 and PTFE/graphene-8 composites (Figure 3a), rapid drops and slow raises can be seen periodically in friction graphs, which can be the influence of transfer layer formation. It is supposed that at a certain transfer layer thickness, the top layer of the transfer film is suddenly removed. Transfer layer formation is then continued on a thinner remaining layer. The duration of the rapid drops was around 2–5 rotational cycles, while the slower increasing periods were around 200–1500 cycles. The friction reduction of the mentioned drops is less than 0.02 [-].

3.2. Wear rate

Figure 4 introduces the wear rate of unfilled and filled PTFE. Neat PTFE had $5.16 \cdot 10^{-4}$ mm³/Nm wear rate against 42CrMo4 steels. PTFE/Al₂O₃-4 polymer samples reached the lowest wear rate which was $2.91 \cdot 10^{-6}$ mm³/Nm. It is more than two orders of magnitude improvement compared to the reference neat PTFE, which is in agreement with the literature [9]. Graphene in 4/8/16 wt% filler content also decreased the wear significantly; their reduction was around 1–2 orders of magnitude, which is in agreement with the literature [10]. PTFE/graphene-4 sample had $4.72 \cdot 10^{-5}$ wear rate.

Our previous research [18, 19] indicates a sufficient material development for BA80 filled composites, which means that most of the functional groups of BA80 are still existing after the sintering process, and the composites have appropriate material properties. In this way, it can be concluded that the functional

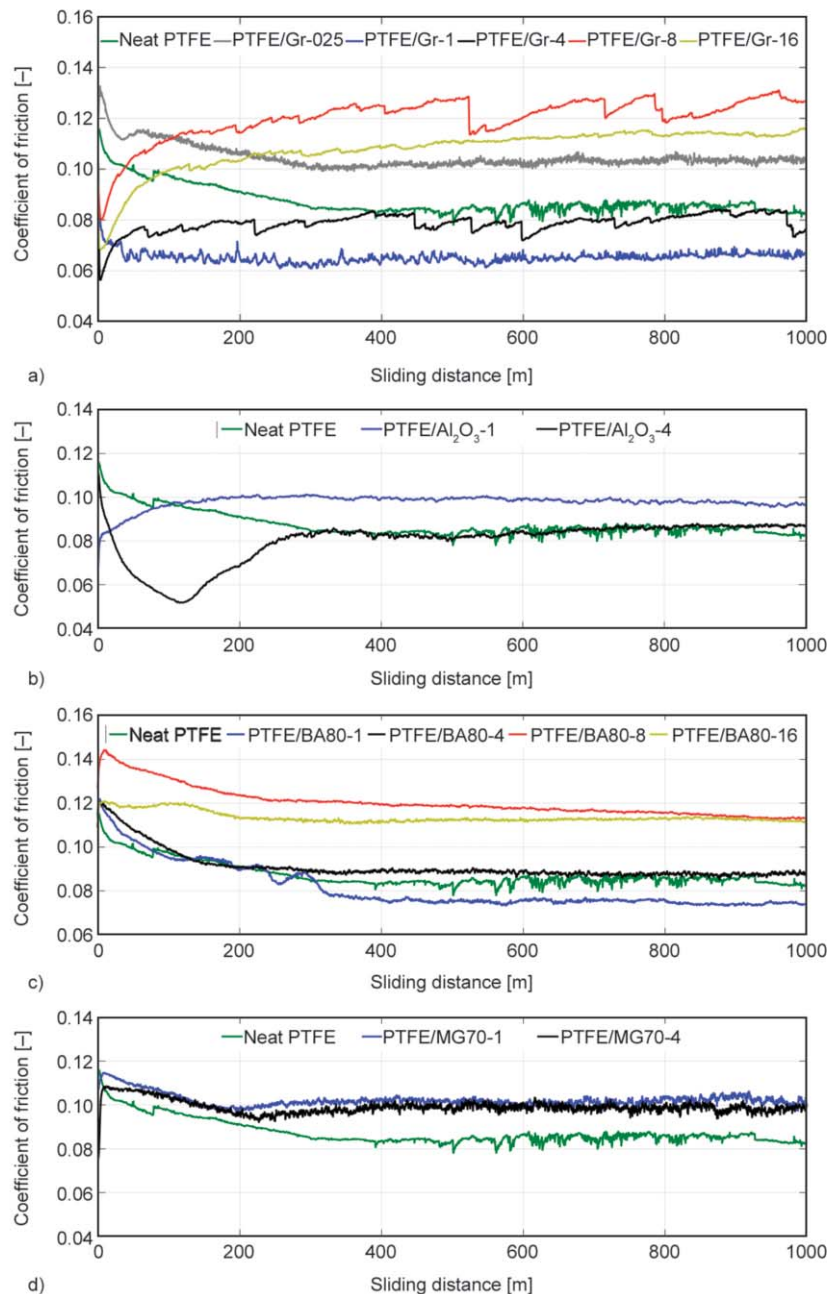


Figure 3. Coefficient of friction graphs of the unfilled/filled PTFE: graphene filled PTFE (a), Al_2O_3 filled PTFE (b), BA80 filled PTFE (c), and MG70 filled PTFE (d).

groups of boehmite did not influence so much the wear rate as it was expected in the research hypothesis. MG70 filled composites did not improve the wear resistance of PTFE. All the tested composites reached the steady-state wear during the 1000 m sliding distance; the observed online wear graphs were linear. Analyses of variance (ANOVA) based on both Bonferroni-Holm and Holm-Šidák methods were evaluated to compare the wear rate of filled PTFE samples to the reference neat PTFE. Both methods concluded that most of the observed differences in the wear rate compared to the reference unfilled PTFE are signif-

icant. Only PTFE/graphene-0.25, PTFE/graphene-1, PTFE/MG70-1, and PTFE/MG70-4 had no significant difference related to the wear rate.

3.3. Transfer layer analysis and wear mechanism

3.3.1. Wear track of the steel counterfaces

Figure 5 displays the macrographs of the tested steel counterfaces for visualization of the formed transfer layer. The macrographs show remarkable differences in the transfer layer formation and the shape and size of the formed debris.

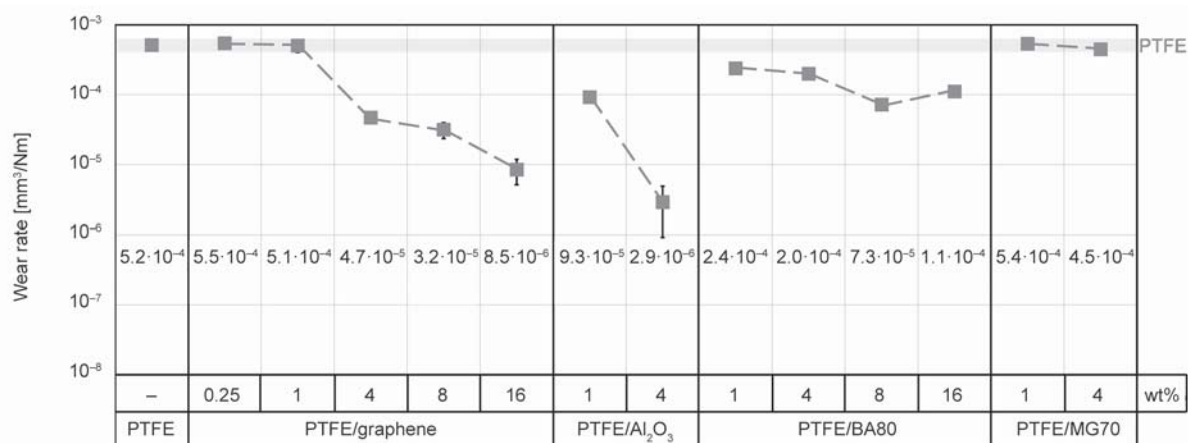


Figure 4. Wear rate of unfilled/filled PTFE samples (based on 5 repetitions, standard deviations correspond to $\pm 1\sigma$, note: the error bars are in logarithmic scale). The grey transparent line displays the measured wear rate of the neat PTFE. Dry contact, 42CrMo4 steel counterface, 3 MPa contact pressure, 0.1 m/s sliding speed, 1000 m sliding distance.

No transfer layer is formed on the surface of the neat PTFE steel disc (Figure 5a). PTFE/graphene-1 and PTFE/BA80-1 steel counterfaces also showed a limited transfer layer formation (Figure 5b and 5f). A more significant transfer layer formation was observed on the surface of PTFE/Al₂O₃-1, PTFE/BA80-4, PTFE/MG70-1 and PTFE/MG70-4 steels (Figure 5d, 5g, 5h and 5i). The surface area of these transfer layers is, however, on the same scale as the formed debris, which indicates that a uniform and durable transfer layer formation was not possible with these materials. On the other hand, PTFE/Al₂O₃-1 composite had a lower wear rate, which comes from the different debris formation mechanisms. As it can be seen in Figure 5d, the size of the formed debris is smaller compared to BA80 or MG70 filled materials, which resulted in a thinner transfer layer as the smaller particles are able to fill the smaller asperity cavities of the steel. PTFE/graphene-4 counterface (Figure 5c) had a partly uniform transfer layer, and the wear debris was smaller than the debris of the PTFE/graphene-1. PTFE/Al₂O₃-4 shows the smallest polymer wear particles (debris) on the steel counterface (Figure 5e), which is in agreement with its ultra-low wear rate. The observed transfer layer of the counterface tested against PTFE/Al₂O₃-4 polymer was uniform, and due to the small debris, the thickness was on the scale of the steel surface asperities.

The transfer layer on the PTFE/graphene-4 counterface was further investigated by white light interferometer (Figure 6). The scale was chosen uniform for a better comparison. The wear track was analyzed in a range of 1.6 mm width. Figure 6a displays the

surface of the unworn steel counterface, while Figure 6b shows the wear track in the steel counterface where significant deposits were detected. Figure 6c introduces the interface of the unworn steel disc (left) and the wear track/transfer layer on the steel (right). This figure can help in making a basic estimation of the thickness of PTFE/graphene-4 transfer layer. The observed results indicate that the thickness of this transfer layer on the steel counterfaces was approximately 1–2 μm .

3.3.2. Wear mechanism of the polymer samples

Figure 7 introduces the surface pattern of PTFE/Al₂O₃-4 polymer pin samples in unworn stage and after 0.1/1/10/100/400 m sliding distance. The results of PTFE/BA80-4 samples were in line with the PTFE/Al₂O₃-4 polymer samples. These two materials were chosen for comparison as they had different transfer layers and debris formation, and a different size of debris. This analysis was carried out with the use of white light interferometry. Figure 7a depicts the rough surface quality of the unworn polymer samples. Their characteristics come from the room temperature pressing. After 10 m sliding distance (Figure 7d), the original surface characteristics disappear, and the dominating surface pattern of the polymer samples becomes similar to the steel counterface. It means that after 10 m sliding distance, the original surface quality of the polymer samples does not affect the sliding process anymore. If the applied sliding distance is 1000 m, the original rough surface quality of the polymer materials can influence the wear process only during the first ~1% of the sliding distance.

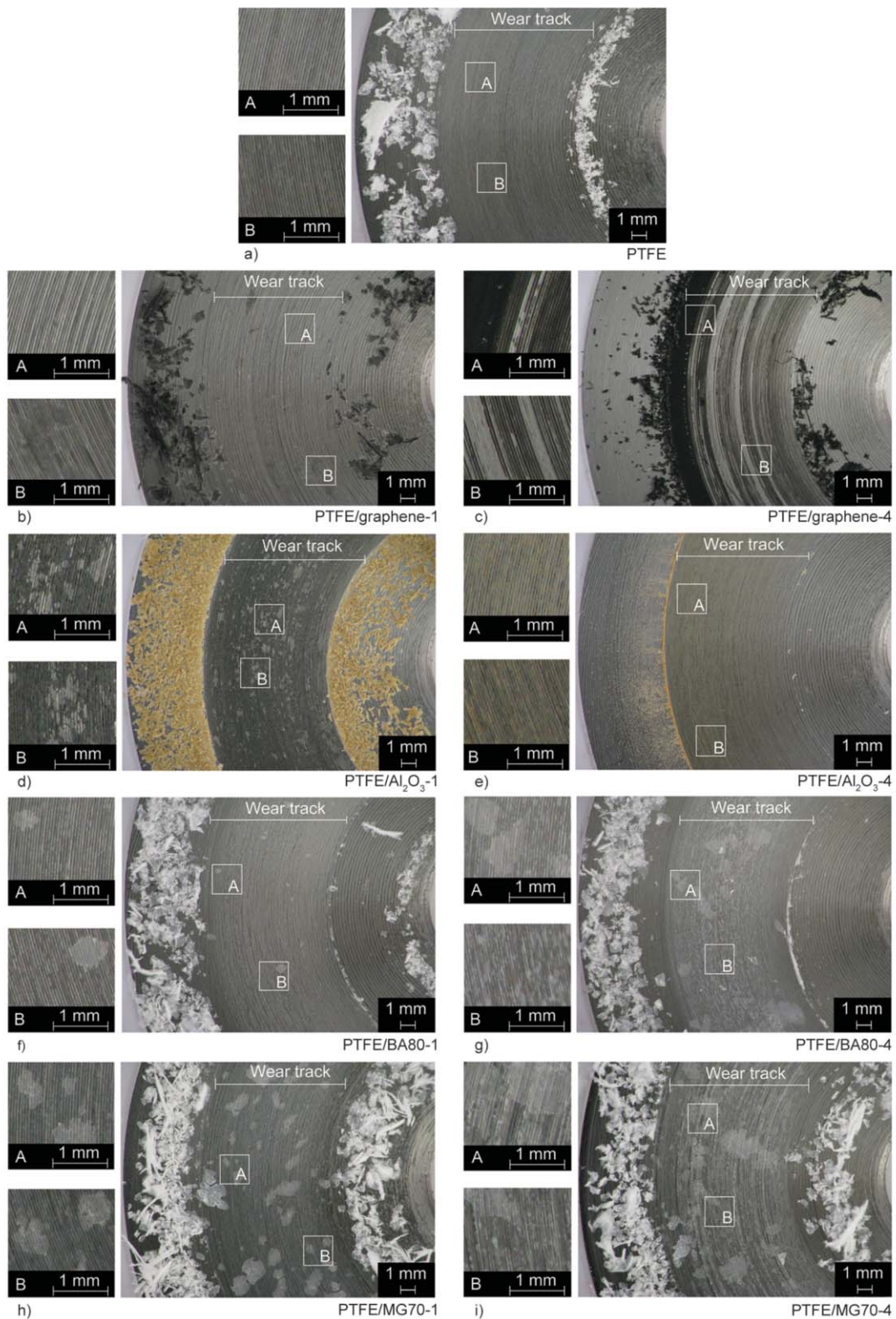


Figure 5. Macrographs of the tested 42CrMo4 counterfaces. Neat PTFE (a), PTFE/graphene-1 (b), PTFE/graphene-4 (c), PTFE/ Al_2O_3 -1 (d), PTFE/ Al_2O_3 -4 (e), PTFE/BA80-1 (f), PTFE/BA80-4 (g), PTFE/MG70-1 (h) and PTFE/MG70-4 (i).

3.3.3. Wear-induced crystallization

The wear-induced crystallization of the unfilled/filled PTFE materials was investigated by DSC. Table 3 introduces the DSC results of the unworn samples and the polymer debris of the worn samples.

The analyzed unworn specimens and the wear debris come from the same polymer sample. The DSC specimens of the unworn material were cut from the opposite (unworn) side of the tested sample. The DSC analysis did not include the debris of PTFE/graphene-8,

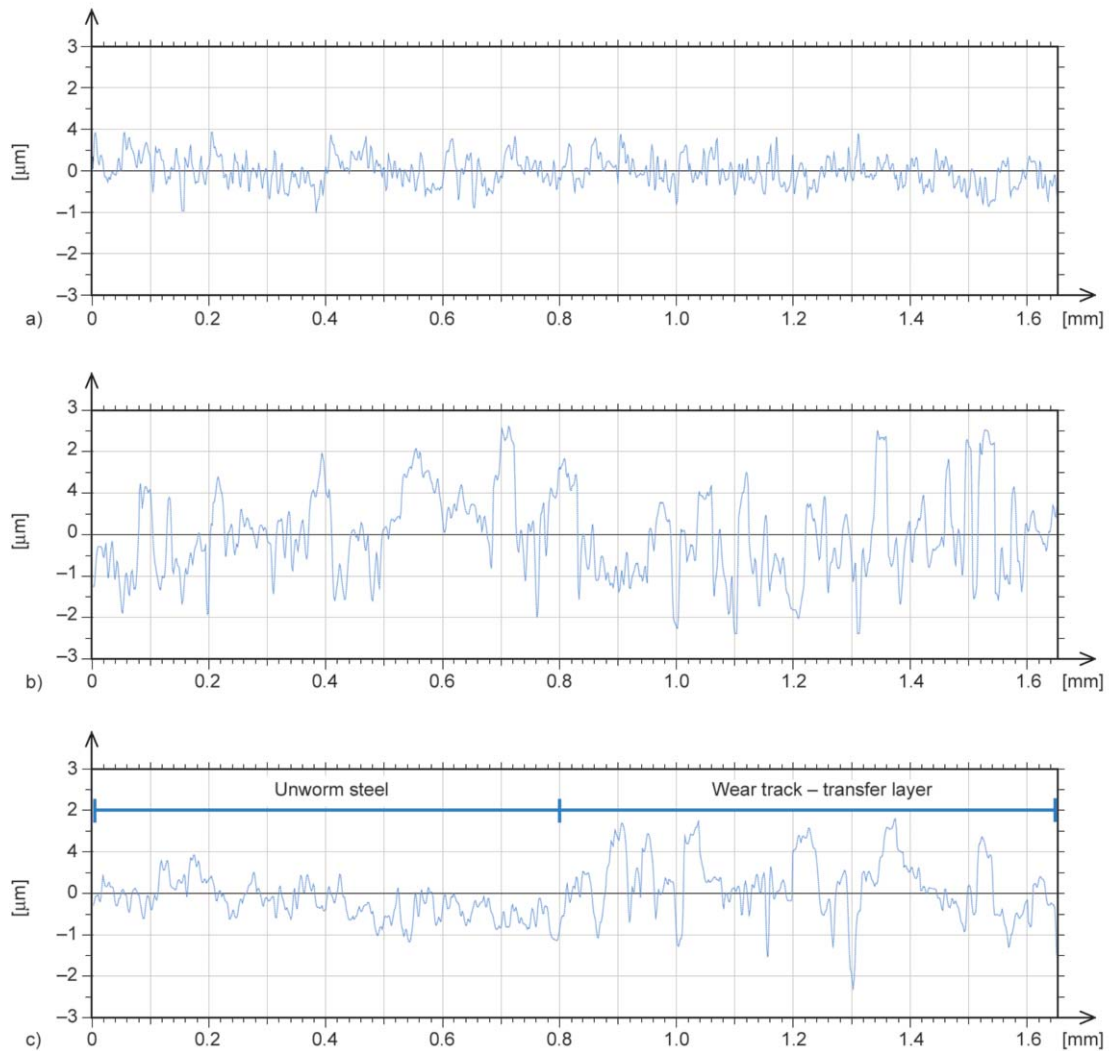


Figure 6. The unworn steel (a), the wear track/transfer layer (b), the interface of the unworn steel, and the transfer layer (c) on the steel counterface tested against PTFE/graphene-4.

PTFE/graphene-16, and PTFE/ Al_2O_3 -4 polymers as these materials had a low wear rate; in this way, the amount of the formed debris was not sufficient for DSC analysis.

In the first heating cycle, the degree of crystallinity of the debris increased between 23 and 35% compared to the unworn samples (Table 3). This increase can come from the different thermal and mechanical antecedents. The surface temperature during wear tests can be so high, which can affect the morphological structure of PTFE materials. Furthermore, the applied pressure and the sliding motion can also align the molecular chains due to the high shear stress during the wear process.

The increase of the degree of crystallinity was also confirmed by the results of the second heating cycle where, after the first melt, all the analyzed samples had the same thermal history. In this way, the thermal history or the molecular chain aligning of the debris

cannot be the reason for this significant increase in the degree of crystallinity. In the second heating cycle, the debris had 24–49% higher degree of crystallinity than the unworn samples (Table 3).

From these results, it can be concluded that this significant increase in the degree of crystallinity comes from the influence of high shear stress during the wear process. It is well known from the literature [9, 10, 12] that during the wear process, the PTFE molecular chains undergo mechanical chain scission. This mechanical chain scission can cause a significant molecular length decrease in the formed debris. These shorter molecular chains of the debris can more efficiently reach an aligned arrangement than the longer chains of the unworn materials. In this way, the degree of crystallinity can be higher not only in the first heating cycle but also in the second heating cycle beside the same thermal history.

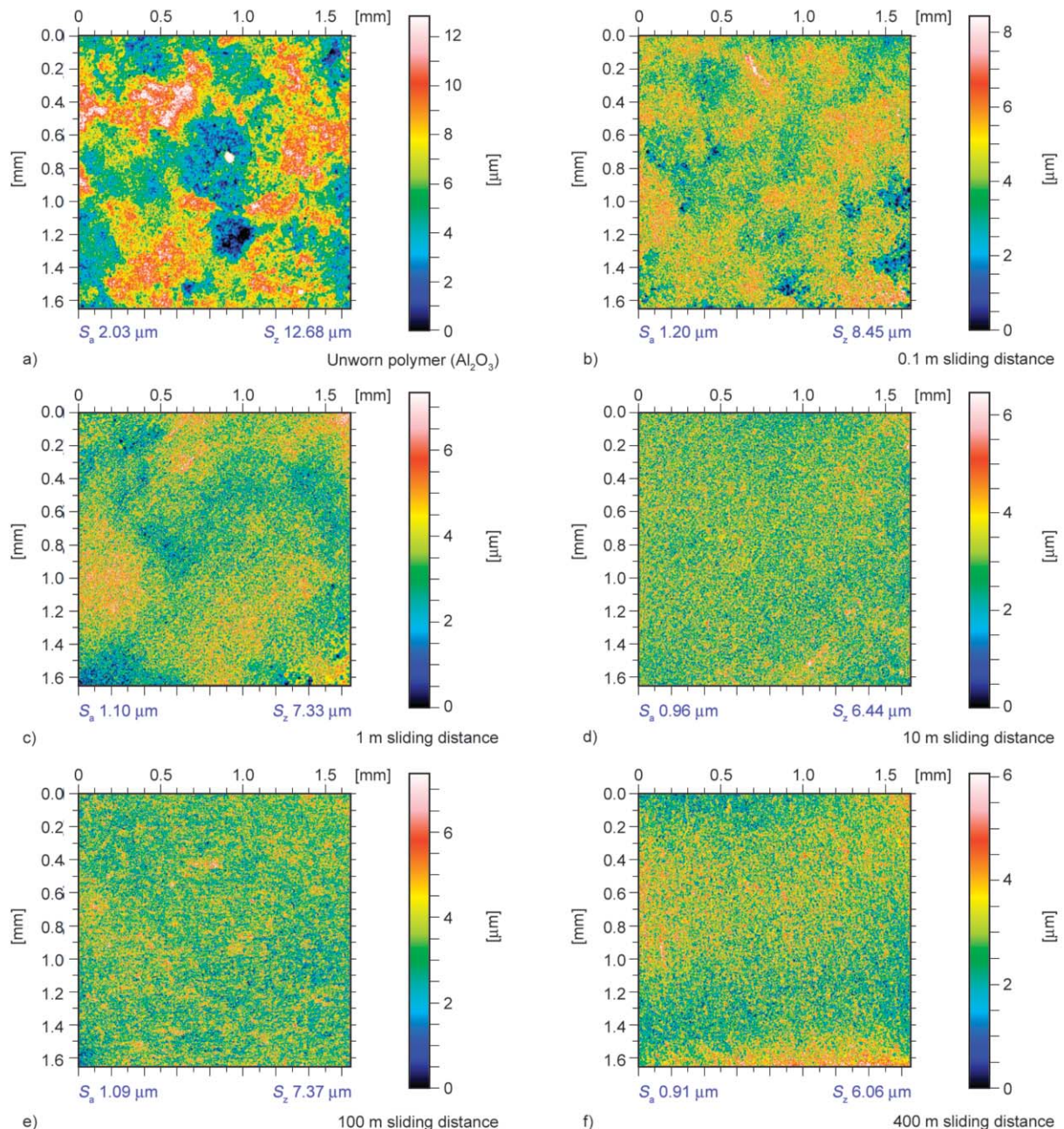


Figure 7. The contact surface of PTFE/Al₂O₃-4 polymer samples against 42CrMo4 steel counterfaces (3 MPa contact pressure, 0.1 m/s sliding speed). (a) unworn polymer (Al₂O₃), (b) 0.1 m sliding distance, (c) 1 m sliding distance, (d) 10 m sliding distance, (e) 100 m sliding distance, (f) 400 m sliding distance.

3.3.4. Filler accumulation in the tested polymers

The aluminum accumulation in the worn polymer surface and debris was investigated by EDS analysis. On the contact surfaces of the worn samples, filler accumulation was observed. In the case of PTFE/Al₂O₃-4 polymer samples, the worn surfaces tested against 42CrMo4 steel discs had ~82% higher aluminum content than the original unworn surfaces. In the case of PTFE/BA80-4 polymer samples, the worn surfaces had ~262% higher aluminum content than the original unworn surfaces. In contrast to this, the

formed debris of PTFE/Al₂O₃-4 polymer samples contains ~82% less aluminum than the original unworn samples. This filler content decrease cannot be seen in the case of PTFE/BA80-4 polymer debris. The EDS analysis of PTFE/Al₂O₃-4 transfer layer on the polymer sample can be seen in Figure 8. Interestingly, Fe content around ~10% was also observed on the polymer contact surface, which comes from the steel counterface. Figure 8c indicates that the lighter areas of Figure 8a have significant Fe content. The reason for this Fe content can be that during

Table 3. DSC analysis of sintered filled/unfilled PTFE samples. Regarding the debris, the enthalpy of fusion at the first heating cycle was evaluated between 300 and 370 °C.

Unworn samples	Degree of crystallinity [%]					
	First heating			Second heating		
	Unworn	Debris	Debris – Unworn	Unworn	Debris	Debris – Unworn
PTFE	53.4	79.1	25.7	43.4	67.5	24.1
PTFE/graphene-0.25	47.2	77.3	30.1	40.2	70.7	30.4
PTFE/graphene-1	51.2	79.0	27.8	43.9	71.9	28.0
PTFE/graphene-4	50.0	84.3	34.4	41.7	79.8	38.2
PTFE/graphene-8	44.9	–	–	41.1	–	–
PTFE/graphene-16	50.3	–	–	43.0	–	–
PTFE/Al ₂ O ₃ -1	51.9	75.2	23.3	41.4	83.0	41.6
PTFE/Al ₂ O ₃ -4	56.2	–	–	48.5	–	–
PTFE/BA80-1	46.8	77.5	30.7	39.8	67.0	27.3
PTFE/BA80-4	47.0	79.7	32.7	40.7	80.5	39.8
PTFE/BA80-8	50.7	78.2	27.5	43.0	80.5	37.5
PTFE/BA80-16	47.9	80.1	32.2	40.3	88.8	48.5
PTFE/MG70-1	40.2	70.2	30.1	35.7	62.3	26.7
PTFE/MG70-4	49.5	84.6	35.1	43.1	74.5	31.4

wear, the hard alumina fillers can damage and partly remove the oxide layer of the steel counterface. On the transfer layer of PTFE/graphene-4, PTFE/BA80-4, and PTFE/MG70-4 polymer samples, no Fe content was registered due to the less hard filler particles and relatively high wear rate of these samples. In other words, after the wear test of PTFE/Al₂O₃-4 polymer,

an extremely low amount of material was removed from the polymer sample. In this way, the contact layer of PTFE/Al₂O₃-4 polymer could collect more Fe without losing the Fe-rich top layer during the wear mechanism of the polymer.

The more significant aluminum and iron content were also confirmed by FTIR spectroscopy (Figure 9a).

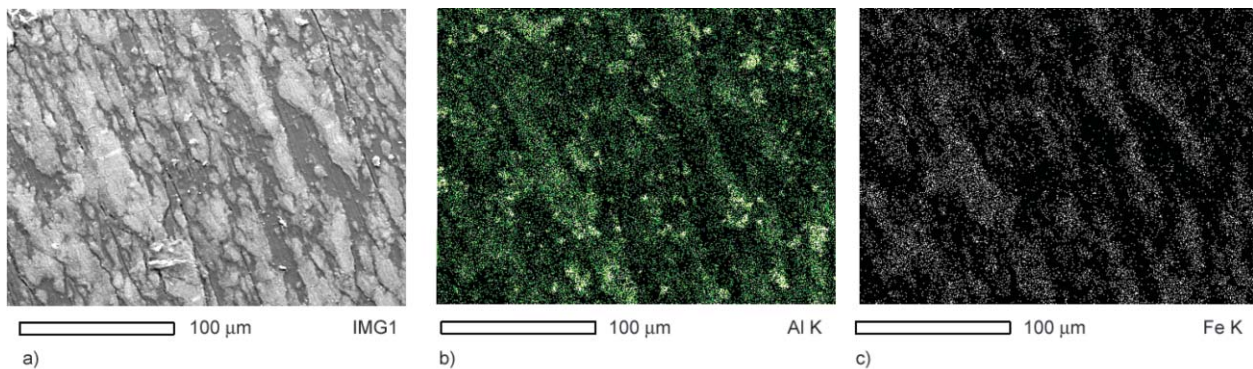


Figure 8. EDS analysis of PTFE/Al₂O₃-4 transfer layer on the polymer surface (42CrMo4 steel counterface, 3 MPa contact pressure and 0.1 m/s sliding speed); micrograph of the transfer layer (a), aluminium content (b) and iron content (c).

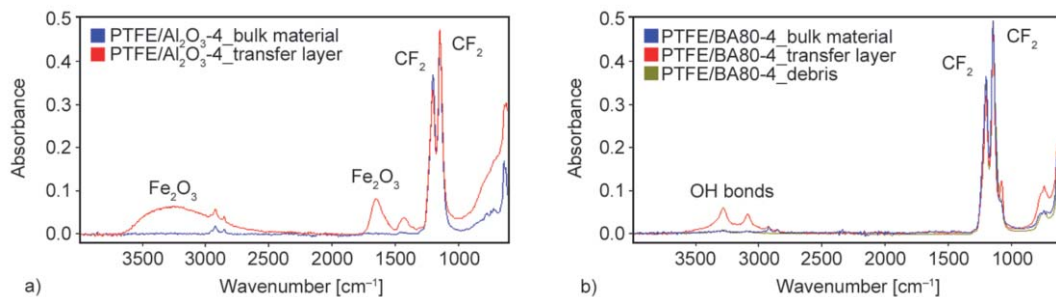


Figure 9. FTIR spectra of PTFE/Al₂O₃-4 (a) and PTFE/BA80-4 (b) polymer bulk materials (blue), transfer layers (red) and debris (olive).

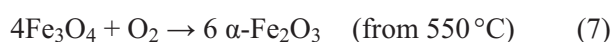
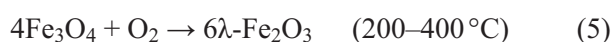
The new peaks from the iron content can only be seen in Figure 9a (PTFE/Al₂O₃-4). The peaks of aluminum bonds are more intensive in the transfer layer (red) than in the bulk material (blue). The hydroxyl (OH) bonds of PTFE/BA80-4 transfer layer (Figure 9b) are also more visible compared to the unworn material due to the filler accumulation.

The filler content of the worn surface of the polymer samples with 0.1/1/10/100/200/400 m sliding distance was analyzed to collect more detailed information about the process of filler accumulation (Table 4). The filler content reached a significant increase even after 10 m sliding distance, and after this 10 m, there is only a slight increase in filler content. It means that almost the total registered accumulation occurs in the first 10 m.

Figure 10 displays the contact surfaces of PTFE/Al₂O₃-4 polymer samples. The original, unworn polymer surface can be seen in Figure 10a, while the worn contact surfaces after 0.1/1/10/100/400 m sliding distance are introduced in Figure 10b–10f, respectively.

In Figure 10b, it can be seen that even after 0.1 m sliding distance, black spots appeared in the polymer contact surface, which comes from the oxide layer of the steel counterface. In Figure 10b–10d, an accumulation of the spots can be observed, which is in agreement with the results of EDS measurements (Table 4). After 10 m sliding distance (Figure 10d–10f)), the black color of iron oxide particles became orange. This change in their color shows that the removed iron oxide particles are modified during the wear process. The black colour indicates that the iron oxide particles include basically Fe₃O₄ (iron(II,III)

oxide) molecules; in other words, the original stage is magnetite. The orange color indicates high Fe₂O₃ (iron(III) oxide) content which means that the iron oxide goes through an oxidation process during wear. Focusing on Fe₂O₃, λ-Fe₂O₃ can be found in maghemite (brown color), and α-Fe₂O₃ is in hematite (red color). Equations (5)–(7) introduce the background of these stages:



These temperature values in Equations (5)–(7) indicate that the local temperature of the contact surfaces during the wear process reached a minimum of 375–400 °C.

In the case of PTFE/BA80-4 polymer samples, none of the contact surfaces included iron according to the EDS and optical measurements as well. It can have two different reasons; the first is that PTFE/BA80-4 sample had a much higher wear rate compared to PTFE/Al₂O₃-4; in this way, the top layer of the polymer with the iron content is removed. Here it is important to mention that even after 0.1/1/10 m sliding distance, no iron content was detected on the PTFE/BA80-4 polymer contact surfaces. In contrast with this, iron content accumulation was registered in the given sliding distances on the PTFE/Al₂O₃-4 contact surfaces. It means that even if a more significant material depth was removed from PTFE/BA80-4 samples, the worn contact surface of these polymers should have some iron content as the iron oxide is

Table 4. EDS analysis results of unworn samples and contact surfaces (3 MPa contact pressure and 0.1 m/s sliding speed).

Materials	Sliding distance [m]	Aluminum content unworn [%]	Aluminum content worn surface [%]	Iron (Fe) content worn surface [%]	Aluminum content = worn/unworn [%]
PTFE/Al ₂ O ₃ -4	0.1	2.54	3.28	0.85	129.1
PTFE/Al ₂ O ₃ -4	1	3.06	4.23	2.59	138.2
PTFE/Al ₂ O ₃ -4	10	3.15	9.06	4.01	287.6
PTFE/Al ₂ O ₃ -4	100	2.91	7.89	3.85	271.1
PTFE/Al ₂ O ₃ -4	200	3.45	10.45	5.26	302.9
PTFE/Al ₂ O ₃ -4	400	3.40	11.31	5.71	332.6
PTFE/BA80-4	0.1	2.01	2.53	~0	125.9
PTFE/BA80-4	1	2.10	2.64	~0	125.7
PTFE/BA80-4	10	1.90	6.34	~0	333.7
PTFE/BA80-4	100	1.89	7.74	~0	409.5
PTFE/BA80-4	200	2.22	7.81	~0	351.8
PTFE/BA80-4	400	1.97	7.40	~0	375.6

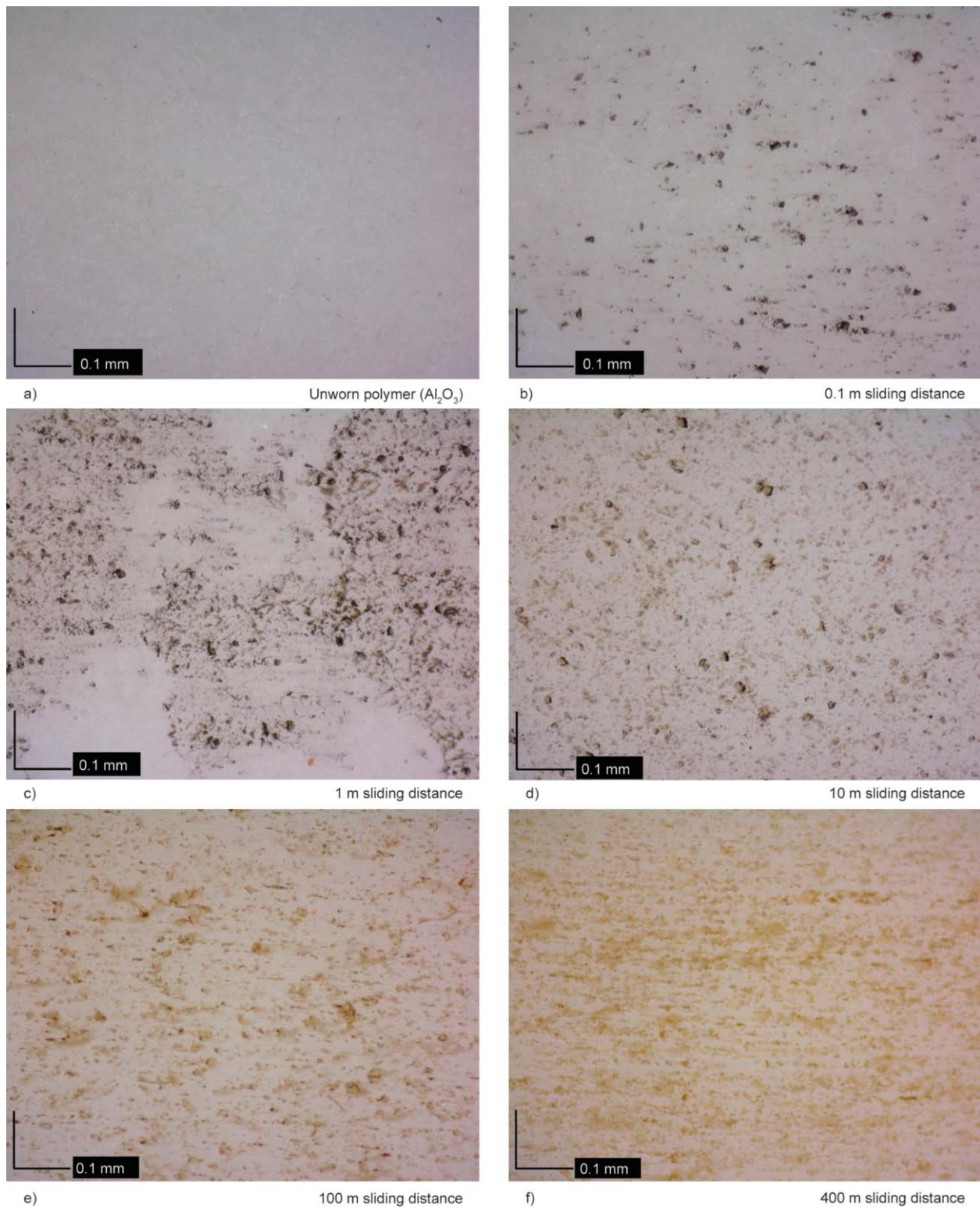


Figure 10. Iron oxide accumulation on PTFE/Al₂O₃-4 polymer contact surface (42CrMo4 steel counterface, 3 MPa contact pressure, and 0.1 m/s sliding speed). (a) unworn polymer (Al₂O₃), (b) 0.1 m sliding distance, (c) 1 m sliding distance, (d) 10 m sliding distance, (e) 100 m sliding distance, (f) 400 m sliding distance.

removed continuously from the counterface. In this way, the second potential explanation is that Al₂O₃ filler contains abrasive and hard particles. These particles can damage and remove the peaks of the steel counterface, resulting in an iron-oxide accumulation

on the polymer contact surface. All kinds of steel surface damage have to be avoided as, in general, the polymer surface (*e.g.*, bearings and seals) is the sacrificial part. In this way, the steel counterfaces were analyzed by white-light interferometry, and at

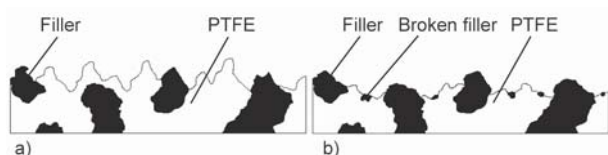


Figure 11. Illustration of wear mechanism and filler accumulation of the top surface; original unworn surface (a) and worn surface (b).

these test conditions, no visible damages, scratches were detected on the contact surfaces.

A potential explanation for the alumina filler accumulation is that the softer PTFE particles can be torn easier from the contact surface than the hard metal oxide filler particles. In this way, the filler content of the contact surface is higher due to the still remaining fillers. Some of the torn or broken filler particles can also stick again as back transfer into the softer PTFE due to the high pressure and high temperature. This mechanism is illustrated in Figure 11. As less filler is removed from the contact surface of the polymer during wear, it is evident that the debris had lower filler content.

4. Conclusions

This research work introduced the friction and wear-characterization and the transfer layer formation of unfilled and mono-filled PTFE.

- PTFE/Al₂O₃-4 samples achieved the lowest wear rate with a decrease of more than two orders of magnitude compared to the neat PTFE. As our previous research work [19] introduced, this ultra-low wear rate cannot be indicated by the modified hardness, compressive/shear/tensile properties, or thermal conductivity.
- The high wear rate improvement of PTFE/Al₂O₃-4 sample comes from the modified transfer layer formation. On the contact surfaces of the worn polymer samples, filler and iron-oxide accumulation was observed, which can serve as a more protective layer. The reason for the high filler accumulation is that the softer PTFE particles can be torn easier from the contact surface than the hard metal oxide filler particles. The broken filler particles can also penetrate back into the softer PTFE due to the high pressure and high temperature. Regarding the iron-oxide accumulation, Al₂O₃ filler contains abrasive and hard particles which can remove the peaks of the steel counterface.
- After 10 m sliding distance, the dominating surface pattern of the polymer samples becomes similar to

the steel counterface. It means that if the sliding distance is 1000 m, the original rough surface quality of the polymer materials can influence the wear process only at the first ~1% of the sliding distance.

- After the wear tests, the degree of crystallinity of the debris increased compared to the unworn samples. This increase comes from the mechanical chain scission in the molecular chains during the wear process. Due to this phenomenon, the molecular length was shortened in the formed debris, which increased the degree of crystallinity.

Acknowledgements

Levente Ferenc Tóth acknowledges the financial support received through ÚNKP-18-3-I-BME-176 New National Excellence Program of the Ministry of Human Resources. This research was performed under a cooperative effort between Ghent University (Belgium) and Budapest University of Technology and Economics (Hungary). The authors would like to thank 3M Company and Azelis for their material support. The authors acknowledge the efforts of Professor József Karger-Kocsis[‡], Beáta Szolnoki, Tamás Igricz and Balázs Pinke from Budapest University of Technology and Economics, and Professor Dieter Fauconnier from Ghent University. The research reported in this paper and carried out at BME has been supported by the NRD Fund (TKP2020 IES, Grant No. BME-IE-NAT) based on the charter of bolster issued by the NRD Office under the auspices of the Ministry for Innovation and Technology.

References

- [1] Song P., Wang C., Chen L., Zheng Y., Liu L., Wu Q., Huang G., Yu Y., Wang H.: Thermally stable, conductive and flame-retardant nylon 612 composites created by adding two-dimensional alumina platelets. *Composites Part A: Applied Science and Manufacturing*, **97**, 100–110 (2017).
<https://doi.org/10.1016/j.compositesa.2017.02.029>
- [2] Liang J-Z.: Effects of tension rates and filler size on tensile properties of polypropylene/graphene nanoplatelets composites. *Composites Part B: Engineering*, **167**, 241–249 (2019).
<https://doi.org/10.1016/j.compositesb.2018.12.035>
- [3] Burk L., Walter M., Asmacher A. C., Gliem M., Moseler M., Mülhaupt R.: Mechanochemically aminated multi-layer graphene for carbon/polypropylene graft polymers and nanocomposites. *Express Polymer Letters*, **13**, 286–301 (2019).
<https://doi.org/10.3144/expresspolymlett.2019.24>
- [4] Rodriguez V., Sukumaran J., Schlarb A. K., De Baets P.: Reciprocating sliding wear behaviour of PEEK-based hybrid composites. *Wear*, **362–363**, 161–169 (2016).
<https://doi.org/10.1016/j.wear.2016.05.024>

- [5] Khumalo V. M., Karger-Kocsis J., Thomann R.: Polyethylene/synthetic boehmite alumina nanocomposites: Structure, thermal and rheological properties. *Express Polymer Letters*, **4**, 264–274 (2010).
<https://doi.org/10.3144/expresspolymlett.2010.34>
- [6] Kalácska G.: An engineering approach to dry friction behaviour of numerous engineering plastics with respect to the mechanical properties. *Express Polymer Letters*, **7**, 199–210 (2013).
<https://doi.org/10.3144/expresspolymlett.2013.18>
- [7] Khedkar J., Negulescu I., Meletis E. I.: Sliding wear behavior of PTFE composites. *Wear*, **252**, 361–369 (2002).
[https://doi.org/10.1016/S0043-1648\(01\)00859-6](https://doi.org/10.1016/S0043-1648(01)00859-6)
- [8] Makowiec M. E., Blanchet T. A.: Improved wear resistance of nanotube- and other carbon-filled PTFE composites. *Wear*, **374–375**, 77–85 (2017).
<https://doi.org/10.1016/j.wear.2016.12.027>
- [9] Krick B. A., Ewin J. J., Blackman G. S., Junk C. P., Sawyer W. G.: Environmental dependence of ultra-low wear behavior of polytetrafluoroethylene (PTFE) and alumina composites suggests tribochemical mechanisms. *Tribology International*, **51**, 42–46 (2012).
<https://doi.org/10.1016/j.triboint.2012.02.015>
- [10] Padenko E., van Rooyen L. J., Wetzal B., Karger-Kocsis J.: ‘Ultralow’ sliding wear polytetrafluoroethylene nanocomposites with functionalized graphene. *Journal of Reinforced Plastics and Composite*, **35**, 892–901 (2016).
<https://doi.org/10.1177/0731684416630817>
- [11] Kandanur S. S., Rafiee M. A., Yavari F., Schrameyer M., Yu Z.-Z., Blanchet T. A., Koratkar N.: Suppression of wear in graphene polymer composites. *Carbon*, **50**, 3178–3183 (2012).
<https://doi.org/10.1016/j.carbon.2011.10.038>
- [12] Harris K. L., Pitenis A. A., Sawyer W. G., Krick B. A., Blackman G. S., Kasprzak D. J., Junk C. P.: PTFE tribology and the role of mechanochemistry in the development of protective surface films. *Macromolecules*, **48**, 3739–3745 (2015).
<https://doi.org/10.1021/acs.macromol.5b00452>
- [13] Padenko E., van Rooyen L. J., Karger-Kocsis J.: Transfer film formation in PTFE/oxyfluorinated graphene nanocomposites during dry sliding. *Tribology Letters*, **65**, 36/1–36/11 (2017).
<https://doi.org/10.1007/s11249-017-0821-0>
- [14] Karger-Kocsis J., Lendvai L.: Polymer/boehmite nanocomposites: A review. *Journal of Applied Polymer Science*, **135**, 45573/1–45573/31 (2017).
<https://doi.org/10.1002/app.45573>
- [15] Lendvai L.: Water-assisted production of polypropylene/boehmite composites. *Periodica Polytechnica Mechanical Engineering*, **64**, 128–135 (2020).
<https://doi.org/10.3311/PPme.13981>
- [16] Pedrazzoli D., Khumalo V. M., Karger-Kocsis J., Pegoretti A.: Thermal, viscoelastic and mechanical behavior of polypropylene with synthetic boehmite alumina nanoparticles. *Polymer Testing*, **35**, 92–100 (2014).
<https://doi.org/10.1016/j.polymertesting.2014.03.003>
- [17] Gumede T. P., Luyt A. S., Müller A. J.: Review on PCL, PBS, and PCL/PBS blends containing carbon nanotubes. *Express Polymer Letters*, **12**, 505–529 (2018).
<https://doi.org/10.3144/expresspolymlett.2018.43>
- [18] Tóth L. F., De Baets P., Szabó G.: Processing analysis of nanoparticle filled PTFE: Restrictions and limitations of high temperature production. *Polymers*, **12**, 2044/1–2044/14 (2020).
<https://doi.org/10.3390/polym12092044>
- [19] Tóth L. F., De Baets P., Szabó G.: Thermal, viscoelastic, mechanical and wear behaviour of nanoparticle filled polytetrafluoroethylene: A comparison. *Polymers*, **12**, 1940/1–1940/17 (2020).
<https://doi.org/10.3390/polym12091940>
- [20] Wang X. Q., Chen D. R., Han J. C., Du S. Y.: Crystallization behavior of polytetrafluoroethylene (PTFE). *Journal of Applied Polymer Science*, **83**, 990–996 (2002).
<https://doi.org/10.1002/app.2279>